Magnetic field effects on spin excitations in the spin-Peierls compound $CuGeO_3$

B. Grenier,[1] L. P. Regnault,[1] J. E. Lorenzo,[2] J. P. Boucher,[3] A. Hiess,[4] G. Dhalenne,[5] and A. Revcolevschi[5]
[1]*Département de Recherche Fondamentale sur la Matière Condensée, SPSMS, Laboratoire de Magnétisme et de Diffraction Neutronique, CEA-Grenoble, F-38054 Grenoble cedex 9, France*
[2]*Laboratoire de Cristallographie, CNRS, BP 166, F-38042 Grenoble cedex 9, France*
[3]*Laboratoire de Spectrométrie Physique, Université J. Fourier Grenoble I, BP 87, F-38402 Saint Martin d'Hères cedex, France*
[4]*Institut Laue Langevin, BP 156, F-38042 Grenoble cedex 9, France*
[5]*Laboratoire de Physico-Chimie de l'Etat Solide, Université Paris-Sud, Bâtiment 414, F-91405 Orsay cedex, France*
(Received 27 March 2000)

Neutron inelastic scattering measurements on an undoped single crystal of $CuGeO_3$ and on a doped crystal $CuGe_{0.997}Si_{0.003}O_3$ are performed in the presence of a magnetic field H up to 12 T. In the present work, a particular attention is given to the effect of H on the low-energy elementary excitations. This investigation is performed in the three different phases of the spin-Peierls system. In the dimerized D phase, the Zeeman splitting of the acoustic magnon branch is evaluated all along the dispersion branch ($0<q\leqslant 1/2$). In the uniform U phase, it is established first that, at finite temperature $T\neq 0$, the low wave vector ($q\rightarrow 0$) spinon modes are little affected by the thermal fluctuations $\delta E_T \simeq T$. Second, the effect of H on the same low-q mode results essentially in a transfer of the fluctuations towards the Zeeman-shifted lower boundary of the spinon continuum. Finally, our measurements on the doped compound establishes that an energy gap occurs in the elementary excitation spectrum of the incommensurate I phase.

I. INTRODUCTION

The spin-Peierls transition (SP) remains one of the most fascinating phenomena in solid state physics. It establishes that a three-dimensional lattice of atoms, subjected to the low-energy quantum fluctuations of an internal low-dimensional spin system, can undergo a distortion at sufficiently low temperature.[1] As a result, drastic changes occur also in the spin system. In particular, energy gaps open in the fluctuation spectrum. The renewed interest in this remarkable effect, established more than twenty years ago on organic materials, is due to the inorganic compound $CuGeO_3$.[2] The high quality of available single crystals has allowed a rather wide set of new experimental investigations.[3] Simultaneously, new theoretical and numerical analyzes have been proposed. Recently, it has been suggested that the initial adiabatic approach,[1] which results in the occurrence of a phonon soft mode at the transition, would not apply to that compound. To explain the observed SP transition in $CuGeO_3$, a nonadiabatic[4] (or ''diabatic''[5]) situation where the transition would be driven by a ''central peak'' appears as a possible and promising alternative. Whatever the actual model, a close relation between the fluctuations of the lattice and those of the spin system is to be expected. Complete knowledge of all these fluctuations is therefore required.[6] In the present work, however, we limit our interest to the magnetic fluctuations. More precisely, we focus on the effects of an external magnetic field H on the low-energy excitations of the spin system. The effect of a field H is of crucial importance in the SP phenomenology.[1] As it is well known, a quasiuniversal phase diagram is obtained as a function of H and T, with three distinct phases, denoted hereafter U, D, and I [see Fig. 1(a)].[3,7] These phases are defined with respect to the lattice structure of the spin system. In the U phase, and within the simplest model, this lattice is composed of uniform chains, and a unique lattice parameter—the distance c between two neighboring spins—needs to be used to describe that structure. In the D phase, the spin chains are dimerized and two parameters, c_1 and c_2, are now needed to define the spin chain structure. In the I phase, the lattice distortion undergoes a periodic modulation along the chains, with a periodicity which depends directly on the uniform magnetization, i.e., on the value of the applied field H. Accordingly, in the I phase, the lattice distortion is generally incommensurate and characterized by the wave vector component (in the chain direction) $d=2\pi\tilde{m}$, where $\tilde{m}$ is the magnetization per spin [$d/2\pi$ is expressed in reciprocal lattice units (r.l.u.) and $\tilde{m}$ is evaluated with respect to the quantum spin value, i.e., $0<\tilde{m}<1/2$]. Due to these different lattice structures, for each phase, a specific spin hamiltonian can be defined. The effects of H analyzed in the present work are common features to all SP systems and therefore they are to be considered as general properties of these models. They should not depend, in an essential way, on the precise Hamiltonian of the spin system. Our experimental investigation relies on neutron inelastic scattering (NIS) measurements. They are performed in presence of a relatively large magnetic field (maximum field value $H=12$ T) and for each phase, new results are presented, which are concerned with the low-energy excitations—and/or fluctuations—of the spin system. They are probed for different wave vectors $\mathbf{Q}$ in the reciprocal space of the compound.

The basic properties of $CuGeO_3$ and the experimental conditions are briefly described in the following section. Most of our results have been obtained in the D phase. These results are discussed in Sec. III. The data obtained in the U and I phases are presented in Secs. IV and V, respectively.

II. $CuGeO_3$ AND EXPERIMENTAL DETAILS

Both the undoped and the Si-doped single crystals $CuGeO_3$ and $CuGe_{1-x}Si_xO_3$ ($x=0.003$), used in the present

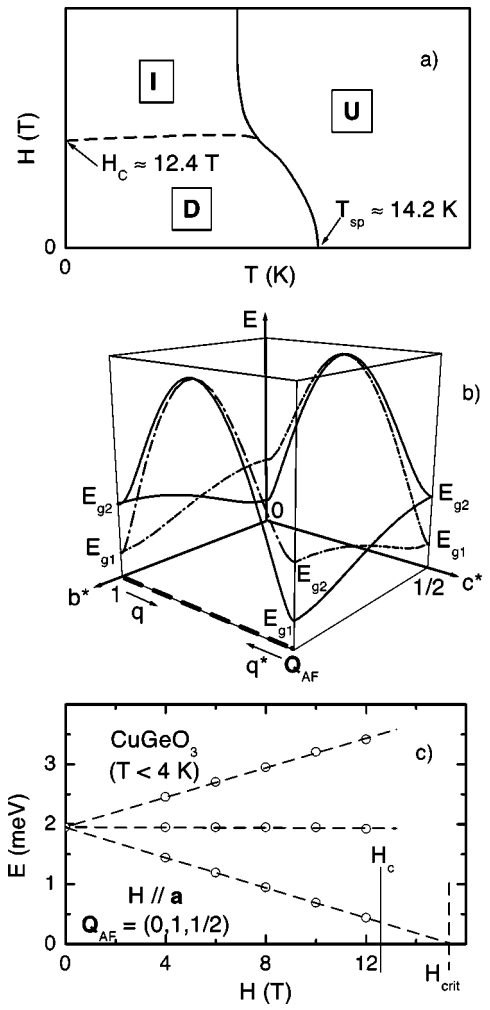

FIG. 1. (a) Experimental phase diagram of $CuGeO_3$ (see Ref. 7 and references therein). (b) Sketch of the energy diagram of the ''magnon'' modes of the *D* phase (in the present work, the small dispersion along the **a*** axis is ignored for simplicity): the solid and dot-dashed lines represent the acoustic and optic branches, respectively. The definitions of q and q^* are shown by the arrows. (c) Zeeman splitting of the acoustic magnon at the AF wave vector $\mathbf{Q}_{\mathrm{AF}}=(0,1,1/2)$ up to $H=12$ T.

study have been grown by a traveling floating zone method associated with an image furnace.[8] They are the same as those used in previous neutron scattering measurements.[9–11] Here, the former crystal is used for the investigation of the *D* and *U* phases, up to $H=12$ T. The presence of defects in a SP system lowers the value of the critical field H_c, which defines the transition between the *D* and *I* phases [see Fig. 1(a)]. For the undoped crystal, $H_c \simeq 12.4$ T. This critical field becomes slightly lower than 12 T in the 0.3%-Si doped compound. The latter crystal is therefore used to probe the *I* phase at $H=12$ T. $CuGeO_3$ crystallizes within an orthorhombic structure of space group *Pbmm*. At 20 K, the lattice parameters of the pure compound are: $a=4.82$ Å, $b=8.41$ Å, and $c=2.94$ Å.[12] The chain axis lies along the **c** axis. Little changes occur in the doped compound. The SP phase diagram for the undoped compound is displayed in Fig. 1(a).[7] In zero field, the transition between the *U* and *D* phases occurs at $T_{sp} \simeq 14$ K. The solid line refers to a second order transition and the dashed line to a first order transition. Along this line, a field-dependent hysteresis is indeed observed at low T (<4 K). In the pure compound, this hysteresis develops in a relatively small field range, $\delta H \simeq 0.08$ T.[13] For the 0.3%-Si compound, δH is larger: $\delta H \simeq 1$ T.[11] The superlattice peak characterizing the lattice dimerization occurring at the $U-D$ transition is defined, in both the undoped and doped compounds, at the wave vector $\mathbf{Q}_{k_{sp}}=(1/2,0,1/2)$. At the *D*-*I* transition, the shift of this superlattice peak towards incommensurate wave vector values has been observed by x-ray[14] and neutron measurements.[11] All these properties are characteristics of the SP phenomenon.

Conventional spin-Peierls theories rely on simple spin models describing purely one-dimensional antiferromagnetic (AF) chains with nearest-neighbor coupling only. If the exchange coupling is assumed to be fully isotropic, the simple following Heisenberg Hamiltonian

$$\hat{H}=J_1^{\parallel}\Sigma_n \mathbf{s}_n\cdot\mathbf{s}_{n+1} \tag{1}$$

can be used, for instance, to describe the magnetic properties of the U phase. In Eq. (1), n labels the spins along a chain and $J_1^{\parallel}$ is the AF intrachain nearest-neighbor magnetic interaction. Magnetic interchain couplings are usually assumed to be very small, $J^{\perp} \ll J_1^{\parallel}$. In $CuGeO_3$, however, this is not the case. As established experimentally,[9,15] they give rise to appreciable dispersions on the low-energy excitation branches [see the simplified representation given for the *D* phase in Fig. 1(b)]. Another important question concerns the presence of a frustrating second nearest-neighbor AF coupling $J_2^{\parallel}$ along the chain.[16] Such a coupling may result from an indirect interaction via the Cu-O-O-Cu bonds.[12] In $CuGeO_3$, it could result also from the expected strong spin-lattice coupling.[4] In that case, it appears as an effective second nearest-neighbor magnetic interaction. In the literature, rather different values have been proposed for $\beta=J^{\perp}/J_1^{\parallel}$ and $\alpha=J_2^{\parallel}/J_1^{\parallel}$. Recent works, however, seem to yield a consensus for the following set of values: $\beta \simeq 0.1-0.15$ and $\alpha \simeq 0.17-0.24$.[17] Magnetic anisotropy is also present in such a real system. In $CuGeO_3$, it is believed to take mainly the form of a Dzyaloshinski-Morya interaction, $d_{\mathrm{DM}}/J_1^{\parallel} \simeq 0.1$.[18] This might explain, in particular, the presence of the second excitation branch—the so-called ''optic'' branch (to be compared to the usual ''acoustic'' branch)—which has recently been observed in the *D* phase.[19] This optic branch is represented by the dot-dashed line in Fig. 1(b). The effective spin hamiltonian for $CuGeO_3$ is certainly quite different from the simple Heisenberg Hamiltonian as expressed in Eq. (1) for the *U* phase. The essential characteristics of the spin-Peierls phenomenon observed in $CuGeO_3$, however, agree qualitatively with the predictions provided by such simple models. The additional couplings, such as $J^{\perp}$, $J_2^{\parallel}$, and d_{DM} mentioned above, seem not to alter in an essential way the basic properties of the low-energy states—in particular, the nature of the ground state and that of the lowest elementary excitations—describing the *U*, *D*, and *I* phases. For the analysis of our data, and as a very first approach, we shall refer in our discussions to such oversimplified spin Hamiltonians.

The NIS measurements to be discussed below have been performed on three different three-axis spectrometers at the Institut Laue-Langevin (ILL) in Grenoble (France): IN12, IN14, and IN8. The two former spectrometers are installed on cold neutron guides. They allow an investigation at low-energy transfers (typically up to about 6 and 10 meV, respectively), with very good wave vector and energy resolutions. The latter spectrometer allows us to extend the investigation to higher energies (up to $\simeq 100$ meV). Different neutron configurations have been used, with final wave vectors kept fixed ($k_f = 1.55$ Å^{-1} on IN12 and IN14; $k_f = 2.662$ Å^{-1} on IN8), with pyrolytic graphite crystals mounted as monochromator and analyzer and with beryllium or pyrolytic graphite filters used to eliminate higher-order contamination. In all cases, the scattering wave vector **Q** was lying in the (b^*,c^*) plane [Fig. 1(b)] and a particular attention has been given to the background which has been accurately estimated for all the scans to be reported. The samples were placed in a split-coil cryomagnet which delivers a vertical field (i.e., applied along the **a** axis of the crystals) up to $H \simeq 12$ T. In the figures showing the neutron data, the scattering wave vector **Q** is given explicitly. However, since we are mainly interested in the behaviors along the chain, we often refer only to the component Q_l as defined along the dashed line in Fig. 1(b). In that case, we use the notations q and q^*, which evaluate the wave vector components from $Q_l = 0$ or $Q_l = 1$ (i.e., $q = |Q_l|$ or $q = |Q_l - 1|$) and $Q_l = 1/2$ (i.e., $q^* = |Q_l - 1/2|$), respectively. The notation q^* is used mainly to describe excitation modes near $\mathbf{Q}_{AF}$ (or near equivalent wave vectors), i.e., excitations sensitive to AF fluctuations, and q is used to describe ''quasiuniform'' fluctuations (along the chains) .

In order to better emphasize the effects of a magnetic field, and also to improve the accuracy of our description, a ''differential analysis'' method has been used in some cases. It consists of performing similar measurements for two different field values while the other experimental conditions are maintained identical. The analysis is made by subtracting the two sets of data. In this way, all the contributions insensitive to H are eliminated (background and possible phonon contributions). An example is reported in Fig. 2, for energy scans performed in the D phase, for $H = 11.8$ T and $H = 0$, respectively. Considering the data in Fig. 2(a), one would conclude that the effect of H results in a simple broadening of the observed magnon mode. The differential analysis reported in Fig. 2(b), however, displays more details. Within a given model, it allows us to develop a more accurate comparison. In the present case, the observed effect corresponds to a Zeeman splitting of the single mode in three distinct lines (see the discussion below). The position and intensity of each line is determined first from Fig. 2(b). Finally, in Fig. 2(a), the reconstitution (shown as the dashed lines) is compared to the initial data.

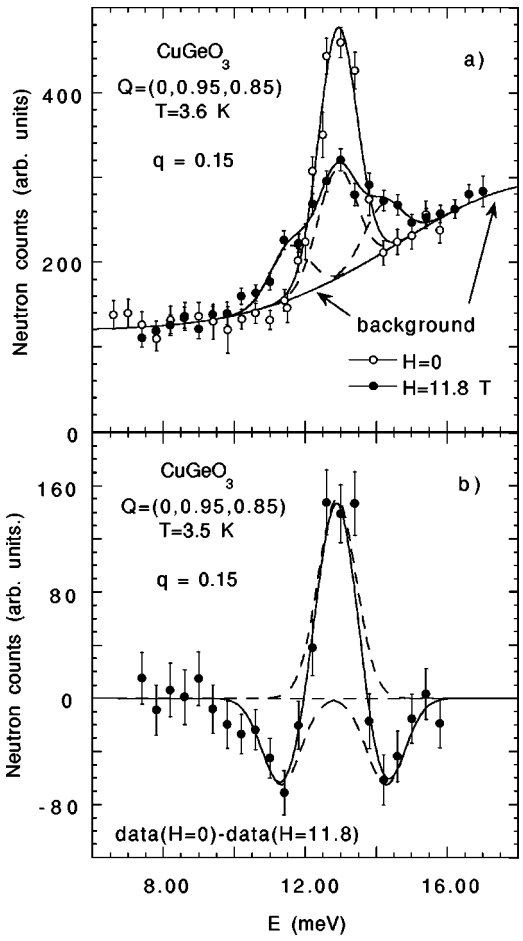

FIG. 2. (a) Field effect on the magnon mode of the D phase at $q = 0.15$ measured at $H = 0$ and 11.8 T on IN8. (b) Differential analysis of the same data [data($H = 0$ T) − data($H = 11.8$ T)]. The background is estimated from low and high-energy data (typically, $E < 10$ and > 16 meV) obtained at several temperatures and fields [see also Fig. 10(a)]. The corresponding line is a polynomial function fitted to these data. The other lines are explained in the text.

III. FIELD EFFECTS IN THE *D* PHASE

As explained above, two lattice parameters, c_1 and c_2, are needed to characterize the structure of a single chain in the D phase. Accordingly, an ''alternation'' occurs in the successive nearest-neighbor exchange couplings along the chains. In its simplest form, the Hamiltonian can be written as

$$\hat{H} = J_1^{\parallel} \Sigma_n [1 + (-1)^n \delta_1] \mathbf{s}_n \cdot \mathbf{s}_{n+1} \tag{2}$$

where δ_1 is the ''alternation'' parameter [$\delta_1 \simeq 0.04$, in $CuGeO_3$ (Refs. 3,9)]. The low-energy properties of such a model are well established.[20] The ground state is nonmagnetic and defined by the quantum number $S = 0$, where **S** is the total spin operator. The lowest excitation branch—hereafter the ''magnon'' branch of the D phase—develops an energy gap, which is defined as a triplet $S = 1$ state. For such a gapped system, the effect of a magnetic field (which defines the z direction) results in a Zeeman splitting and three distinct magnon branches with respective quantum spin numbers $S_z = 0$, $+1$, and -1 should occur.[20] Such a Zeeman effect on a magnon mode has been well observed in $CuGeO_3$ by NIS.[10,21] The previous investigations on the spin dynamics, however, were restricted to the AF wave vector $\mathbf{Q}_{AF} = (0,1,1/2)$ (i.e., $q^* = 0$) and to field values lower than $H = 6$ (Ref. 21) and 10 T,[9] respectively, i.e., to values appreciably lower than the critical field H_c ($\simeq 12.4$ T for the ''undoped'' sample). A first important question concerns the behavior of the excitations when the critical field H_c is approached. Are precursor effects—i.e., for instance, a de-

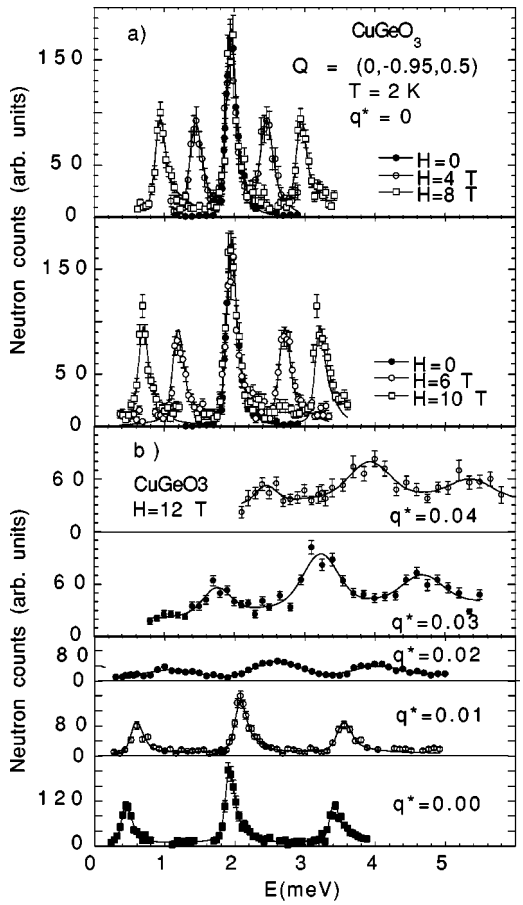

FIG. 3. Fields effects on the magnon modes of the D phase measured on IN12. (a) Very near the AF wave vector $\mathbf{Q}_{\mathrm{AF}}=(0,1,1/2)$, i.e., $q^*=0$ (for $H=0$, the counting is half of that for $H\neq 0$). (b) For $q^*\geqslant 0$ at $H=12$ T, up to $q^*=0.04$. The lines are guides to the eye. The broadening observed with q increasing is entirely due to the instrumental resolution.

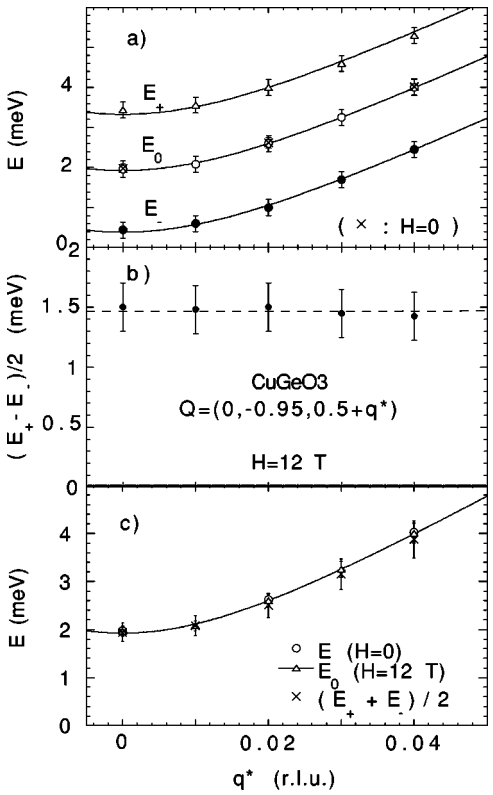

FIG. 4. IN12 measurements at $H=0$ and $H=12$ T. (a) Dispersion curves of the three Zeeman split magnon modes (E_+, E_0, and E_-) of the D phase for low-q^* values. (b) Average energy difference $(E_+-E_-)/2$ as a function of q^*. (c) Average value $(E_+ +E_-)/2$ as a function of q^*. The solid lines are fits from Eq. (3) (see text)

viation from the linear Zeeman splitting—observed near H_c? Such a result is of importance to check on the dynamics the ''first-order'' character of the $D-I$ transition.[1] A second general question is related to the isotropic nature of the magnetic couplings. For a fully isotropic spin system, one expects the Zeeman splitting to occur in the whole Brillouin zone, i.e., at any wave vector. In presence of magnetic anisotropies, however, the three split branches could collapse in a single branch for wave vectors $\mathbf{Q}\neq\mathbf{Q}_{\mathrm{AF}}$, $(q^*\neq 0)$ as it is commonly observed in gapped anisotropic Haldane $S=1$ spin chains.[22]

The energy scans shown in Figs. 3(a) and 3(b) have been obtained on the instrument IN12. Figure 3(a) (upper and lower panels) displays, with great accuracy, the Zeeman splitting of the acoustic magnon branch at $\mathbf{Q}_{\mathrm{AF}}$ (i.e., $q^*=0$). Three narrow peaks are very distinctly observed up to $H=12$ T, and from the peak positions an accurate evaluation of the Zeeman splitting can be obtained. As shown in Fig. 1(c), where the peak values are reported, no appreciable deviation from the linear field dependence of the Zeeman splitting is detected up to $H=12$ T, i.e., at about 3% from the critical field H_c. If one extrapolates the observed behavior beyond H_c, one obtains that the gap would close at a much larger field $H_{\mathrm{crit}}\simeq 15.4$ T. In $CuGeO_3$, the D-I transition merges well before a second-order transition takes place at H_{crit}. In the present measurements, the linewidth of the observed peaks is entirely controlled by the instrumental resolution, which appears to be less than $\delta E\simeq 0.15$ meV [full width at half maximum (FWHM)]. Near H_c, no additional broadening of the mode at $\mathbf{Q}_{\mathrm{AF}}$ (due to possible precursor critical fluctuations) is observed. These two particular results on the spin dynamics—no deviation in the Zeeman splitting and no appreciable damping—support very well the first order character of the field-induced D-I transition. Figure 3(b) displays, for $H=12$ T and for wave vectors $q^*\leqslant 0.04$, the development of the Zeeman splitting along the reciprocal chain axis. The q^* dependence of the three branches at $H=12$ T is reported in Fig. 4(a), together with that of the single excitation branch observed in zero field (on the same instrument). The q^* dependence of the energy splitting is analyzed in Figs. 4(b) and 4(c). As shown in Fig. 4(b), for each q^* value, the average energy difference $(E_+ -E_-)/2$ between the highest and the lowest branches remains constant. Moreover, the average values $(E_+ +E_-)/2$ [see Fig. 4(c)] coincide precisely with the values E_0 of the $S_z=0$ branch and with those of the $H=0$ triplet branch. Within the experimental accuracy, the field-induced splitting appears to be practically q^* independent, at least in that small q^* range, i.e., $0\leqslant q^*\leqslant 0.04$. As shown by the solid lines in Figs. 4(a) and 4(c), the three observed dispersions are well described by the following expression:

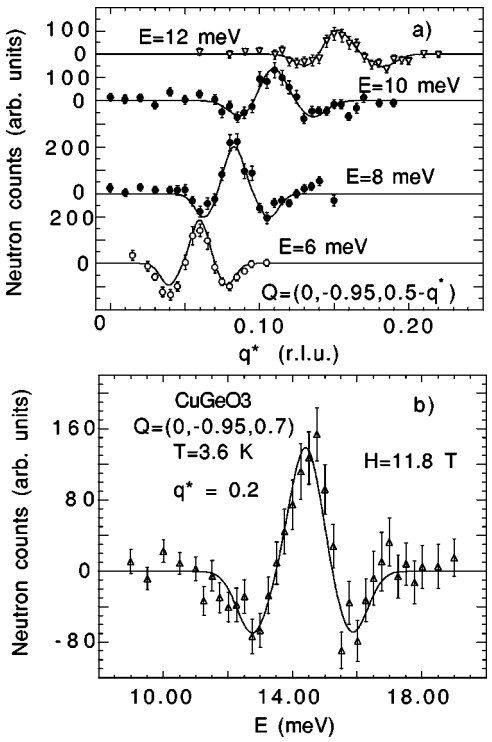

FIG. 5. Fields effects ($H=11.8$ T) on the magnon mode of the D phase measured on IN8, analyzed by the differential method [data($H=0$ T) − data($H=11.8$ T)]. (a) q^* scans at different fixed energies. (b) Energy scans at a fixed wave vector $q^*=0.2$. The lines are fits through the data from the three Zeeman-split magnon model (see text).

$$E^{S_z}(q^*)=\sqrt{[E_{g1}^2+(2\pi q^* C_m)^2]}+\Delta E_z S_z \qquad (3)$$

with $S_z=0$, $+1$ and -1 and where $E_{g1}=1.9$ meV is the SP energy gap, $C_m=13.9$ meV/r.l.u., the (low-q) magnon velocity, and $\Delta E_z=g\mu_B H=1.47$ meV, the Zeeman energy for $H=12$ T.

In order to follow the Zeeman splitting in a larger q range, i.e., at higher energies, NIS measurements at 12 T have been performed on the instrument IN 8. To achieve accurate evaluations, the differential analysis method is systematically applied. The results for $H=11.8$ T with respect to the $H=0$ data obtained from q^* scans at constant energy are displayed in Fig. 5(a). For constant q^* values, the results from energy scans are reported in Figs. 2(b) and 5(b), for $q=0.15$ and $q^*=0.2$ r.l.u., respectively. Our analysis relies on the description established above within our low q^* measurements: the Zeeman splitting results in three distinct modes, each of them being described by a simple Gaussian function whose width is determined by the instrumental resolutions (i.e., no field effect on the widths). As shown by the solid lines, the fitting procedure based on this model reproduces the data very well. The energy of the $S=1$ triplet branch is first determined from the zero field measurements. For $H\neq 0$, the energy E_0 of the $S_z=0$ branch is fixed to the previous values, while E_+ and E_- are considered as adjustable parameters. The values obtained for E_0, E_+ and E_- are reported in Fig. 6 as a function of q^*. The solid lines reproduce very well the observed behavior. They are obtained from the following expression:

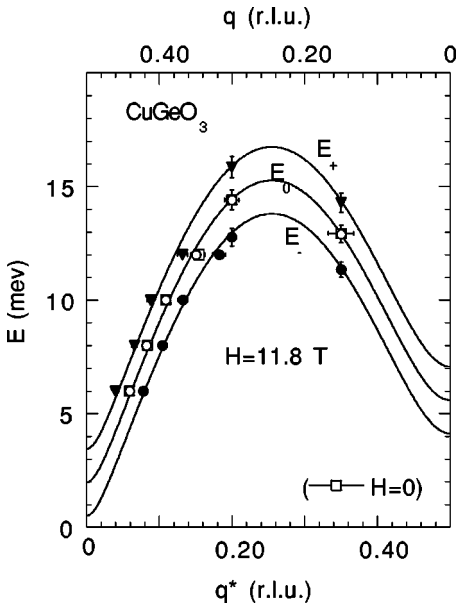

FIG. 6. IN8 measurements at $H=11.8$ T: Dispersion curves of the three Zeeman-split magnon modes (E_+, E_0, and E_-) of the D phase for large q^* values. The lines are fits from Eq. (4) (see text). The data for $H=0$ are also shown.

$$E^{S_z}(q^*)=C_m\sqrt{[1+(1-E_{g2}^2/2C_m^2)\cos(2\pi q^*)]}\times\sqrt{[1-(1-E_{g1}^2/2C_m^2)\cos(2\pi q^*)]}+\Delta E_z S_z \qquad (4)$$

with $C_m=15.3$ meV/r.l.u. and $E_{g2}=5.6$ meV. This equation is an extension of Eq. (1). It applies to $0\leqslant q^*\leqslant 1/2$ and takes into account the presence of a second energy gap E_{g2} at $q^*=1/2$ [$\mathbf{Q}=(1,0)$ in Fig. 1(b)].[23] It is worth noting, however, that the value of the magnon velocity C_m obtained from Eq. (4) is larger than the value obtained from Eq. (3). As discussed in Ref. 3, the smaller magnon velocity evaluated at small q^* values is to be attributed to the second-nearest neighbor Heisenberg coupling $J_2^{\parallel}$ ($\alpha\simeq 0.17$) (see also Ref. 24). It is established here that, in spite of the magnetic anisotropy, the Zeeman splitting develops all along the dispersion branch, with a q^*-independent Zeeman energy ΔE_z ($\simeq 1.47$ meV for $H\simeq 12$ T). To describe the elementary excitations in $CuGeO_3$, the spin components, $S_z=0$, $+1$ and -1, can be considered as good quantum numbers in the whole Brillouin zone.

IV. FIELD EFFECTS IN THE *U* PHASE

As a first approach, to discuss the properties of the U phase, we refer to the simple isotropic Heisenberg spin chain model given by Eq. (1). In the quantum regime of such a model, i.e., at temperatures $T<T_{\max}$, where $T_{\max}$ is defined by the maximum in the susceptibility [$T_{\max}\simeq 60$ K in $CuGeO_3$ (Ref. 2)], the low-energy magnetic fluctuations are known to be described by propagative excitations associated with a continuum, the so-called spinon continuum.[25,26] In zero field, the corresponding spectrum is commensurate with the lattice periodicity [see Fig. 7(a)]. In a field H, however, a dynamical incommensurability develops in the spectra as shown in Figs. 7(b) and 7(c), for the longitudinal (i.e., ob-

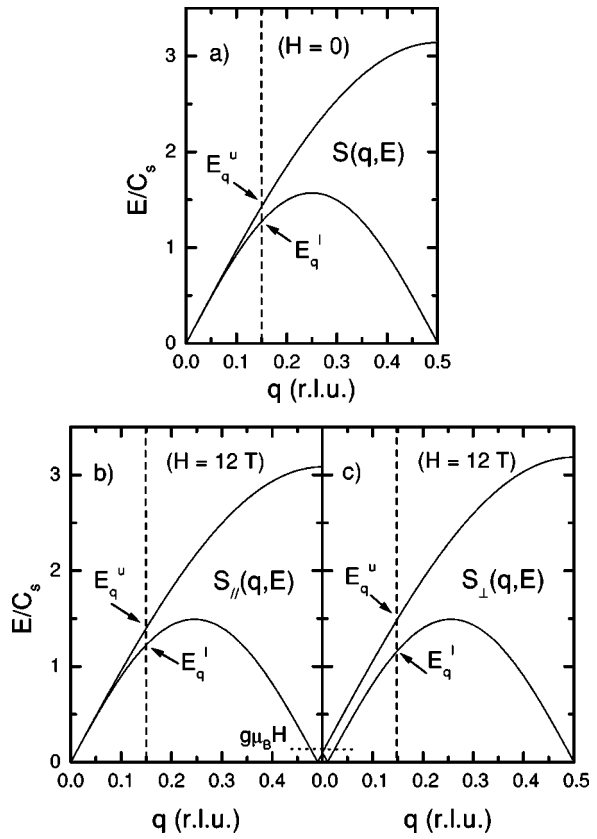

FIG. 7. Sketch of the spinon continuum (at $T=0$) corresponding to the Hamiltonian given in Eq. (1): (a) $H=0$, (b) and (c) $H=12$ T for the longitudinal $S_{\parallel}(q,E)$ and transverse $S_{\perp}(q,E)$ fluctuations, respectively. E_q^u and E_q^l define the upper and lower boundaries of the spinon continuum. C_S represents the velocity of the spinon modes.

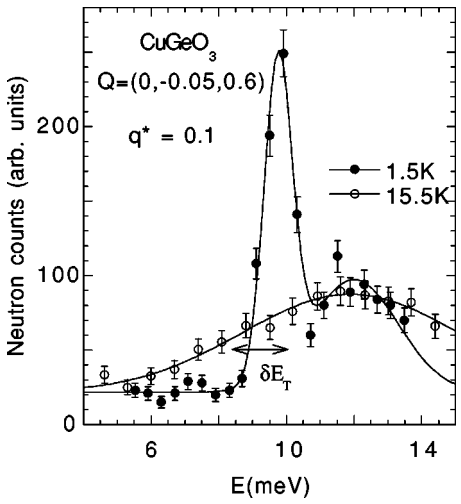

FIG. 8. Magnon and spinon modes (data at 1.5 and 15.5 K, respectively) at $q^*=0.1$ measured on IN8. The lines are guides to the eye. $\delta E_T \simeq T$ evaluates the thermal damping at 15.5 K.

served in the field direction) and transverse fluctuations $S_{\parallel}(q,E)$ and $S_{\perp}(q,E)$, respectively.[25] Such an incommensurability in the spin fluctuations plays a crucial role in the field dependence of the SP transition.[1] For relatively large field values, typically for $H \geqslant H_c$, this dynamical incommensurability in the U phase is expected to drive the incommensurate lattice distortion occurring at T_{SP}. In the U phase, however, since the temperature is never small, $T > T_{SP} \simeq 10-14$ K, the thermal fluctuations cannot be ignored. As established in Ref. 27, at a finite temperature T, the thermal fluctuations are expected to result in an appreciable energy damping ($\delta E_T \simeq T$). This damping is expected to develop essentially at the low-energy boundary of the spinon modes.[28] It is worth noting, however, that, if such a damping acts effectively on the spinon modes sensitive to the AF fluctuations, i.e., near $q=1/2$ ($q^*=0$), it should not affect the uniform spinon modes, i.e., near $q=0$ (as a consequence of the isotropic character of the Heisenberg Hamiltonian).[29] Experimentally in $CuGeO_3$, the effect of such a thermal damping (δE_T) at $q^*=0$ has already been discussed.[3] Another example is reported in Fig. 8, where a comparison between excitations in the D phase (the data at 1.5 K) and in the U phase (the data at 15.5 K) is presented for the same wave vector $q^*=0.1$ ($q=0.4$). In the D phase, the acoustic magnon mode is well defined. It is peaked at $E_q^m \simeq 10$ meV and followed by a broad contribution, which is to be attributed to the two-magnon continuum.[24] As expected, this continuum is shifted from the magnon branch by the energy gap $E_{g1} \simeq 1.9$ meV. In the U phase, however, only a single and broad contribution is observed. It describes the spinon continuum at its low-energy boundary. No well-defined peak is observed and the slow decrease observed at low energies results from the thermal damping: $\delta E_T \simeq 1.34$ meV. At this point, an important comment can be done concerning the ''longitudinal'' fluctuations (i.e., those which develop in the field direction, see below). They are expected to drive the incommensurate lattice distortion below T_{SP}. Due to the thermal damping, however, the dynamical incommensurability on these fluctuations becomes effective only in sufficiently large fields ($H > H_c$), when the Zeeman energy overcomes the thermal fluctuations ($g\mu_B H \geqslant k_B T$).

Let us now focus on the spinon modes associated with small wave vectors ($q \to 0$). According to the spinon model,[25] the intensity of the q modes is predicted to decrease rapidly as $q \to 0$. For this reason, our investigation is limited to the value $q=0.15$. For that wave vector, a comparison between the magnon mode of the D phase (the data at 3.6 K) and the spinon mode of the U phase (the data at 16.2 K) is presented in Fig. 9. The data in the D phase are described by a well-defined single gaussian peak centered at $E_q^m \simeq 12.9$ meV. As before, there is also the two-magnon continuum shifted up by about E_{g1}. At such a low-q value, however, the intensity of this continuum is very small and its contribution becomes negligible.[24] The FWHM of the observed peak ($\delta E_q^m \simeq 1.27$ meV) is mainly determined by the instrumental resolution (for that experimental configuration). When compared to the D phase, one observes that the peak in the U phase is slightly shifted to a lower energy ($E_q^s \simeq 12.5$ meV). An appreciable broadening is also observed on the spinon mode: $\delta E_q^s \simeq 1.70$ meV. From the shift, one establishes a first result: the velocity of the elementary excitations appears to be slightly different in the D and U phases, the (''high-q*'') velocity of the magnon mode ($C_m \simeq 15.3$ meV/r.l.u.) being roughly 4% larger than that of the spinon mode, i.e., $C_s \simeq 14.7$ meV/r.l.u. Second, the observed broadening raises an interesting and basic question. It

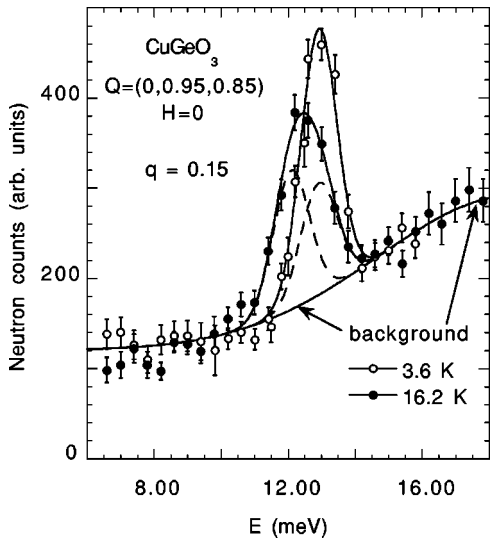

FIG. 9. Magnon and spinon modes (data at 3.6 and 16.2 K, respectively) at $q^*=0.15$ measured on IN8. The solid and dashed lines are gaussian functions (see text). The background is estimated as in Fig. 2(a).

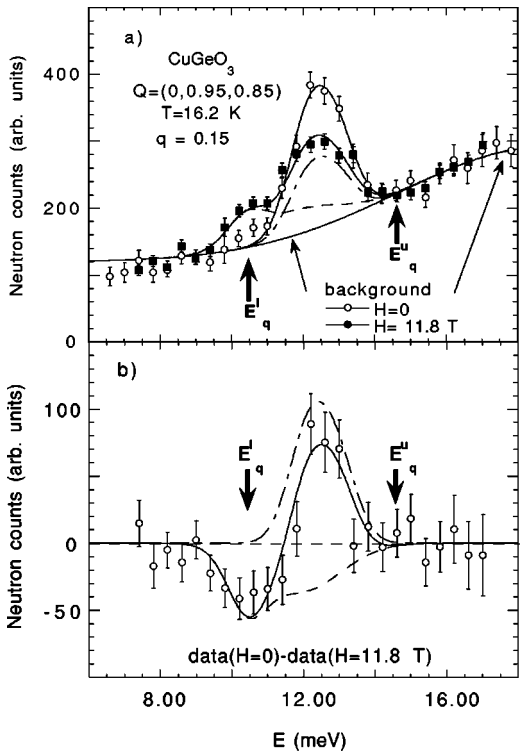

FIG. 10. (a) Field effects on the spinon mode of the U phase measured (at $H=0$ and 11.8 T) on IN8 at $q=0.15$. (b) Differential analysis of the same data [data($H=0$ T) − data($H=11.8$ T)]. E_q^u and E_q^l show the expected upper and lower boundaries of the spinon continuum. The background is defined in the caption of Fig. 2. The other lines are explained in the text.

could be attributed either to the thermal fluctuations (for $T=16.2$ K, $\delta E_T \simeq 1.42$ meV) or to the spinon continuum, which, for that q value, still has an appreciable extension [see Fig. 7(a)]. As a rough approximation, we simply describe the continuum by two gaussian functions (the dashed lines in Fig. 9), with widths equal to that measured on the magnon mode in the D phase ($\delta E_q^m \simeq 1.27$ meV). As shown by the resulting solid line, this simple model reproduces well the observed line shape. From the energy values at which the Gaussian functions are peaked, one obtains an experimental evaluation of the boundaries of the spinon spectrum: for $q=0.15$, the lower- and upper-energy boundaries would be $E_q^l \simeq 12.1$ meV and $E_q^u \simeq 12.9$ meV, respectively. These evaluations are in reasonable agreement with the expectation[25] $E_q^l = C_s \sin(2\pi q) = 11.9$ meV and $E_q^u = 2C_s \sin(\pi q) = 13.3$ meV (assuming $C_s = 14.7$ meV/r.l.u. as determined above). The observed full width of the spinon mode appears to be well explained by the spinon continuum. At such high temperature ($T=16.2$ K), the thermal fluctuations do not affect appreciably the low-q spinon modes of the uniform phase, in agreement with the remarkable prediction[29] established for the simple Hamiltonian in Eq. (1). At this point, a remark should be made about the Gaussian peaked at E_q^u. It is to be related to the recent observation[30] that, in $CuGeO_3$, such a pronounced peak at the upper boundary of the spinon continuum seems to occur in the whole Brillouin zone (see also Ref. 31). For the fully isotropic Hamiltonian in Eq. (1), such a peak is rather unexpected. The presence of a strong XY-like magnetic anisotropy could explain such a behavior.[25] In Ref. 30 it is suggested that it is a consequence of the second next-neighbor exchange coupling $J_2^{\parallel}$. Despite this ''anomaly,'' we believe that the concept of a spinon continuum—a ''modified'' spinon continuum actually—still applies to the U phase of $CuGeO_3$.

The effect of a magnetic field ($H=11.8$ T) on the spinon mode at the same wave vector ($q=0.15$) is displayed in Fig. 10(a). In Fig. 10(b), the same data are analyzed within the differential method. The high field data are compared to the data obtained in zero field. On the two figures, one observes that, upon a field, a large part of the fluctuation spectrum is transferred to lower energies. As explained in Figs. 7(b) and 7(c), due to H, the longitudinal and transverse spinon fluctuations behave differently. At $q=0.15$, the effect of H ($\simeq 12$ T) on the longitudinal fluctuations is negligible [compare Figs. 7(a) and 7(b) for this q value]. The transverse fluctuations are, however, very much affected [Fig. 7(c)] the high- and low-energy boundaries of the spinon continuum should be, respectively, shifted up and down by about the Zeeman energy, i.e., by $\delta_{\pm} = \pm g\mu_B H \simeq \pm 1.45$ meV.[25] Accordingly, the lower and upper limits of the spinon continuum are now expected at $E_q^l \simeq 10.4$ meV and $E_q^u \simeq 14.8$ meV, as shown by the arrows in Figs. 10(a) and 10(b). At $\mathbf{Q}=(0,0.95,0.85)$, where the measurements were performed, the longitudinal and transverse fluctuations contribute almost equivalently to the observed scattering. The contribution of the longitudinal fluctuations (which is not affected by H) can therefore be described by the same function as in zero field (in Fig. 9, the solid line for the 16.2 K data), but with half intensity [the dot-dashed lines in Figs. 10(a) and 10(b)]. The remaining contribution (the dashed lines in those figures) is to be considered as describing the transverse fluctuations only. The maximum in Fig. 10(a) or the minimum in Fig. 10(b) observed at low energy agrees very well with E_q^l. Surprisingly, there is no peak around E_q^u. In these measurements, one observes that the main effect of H is to transfer the fluctuations to the low-energy part of the

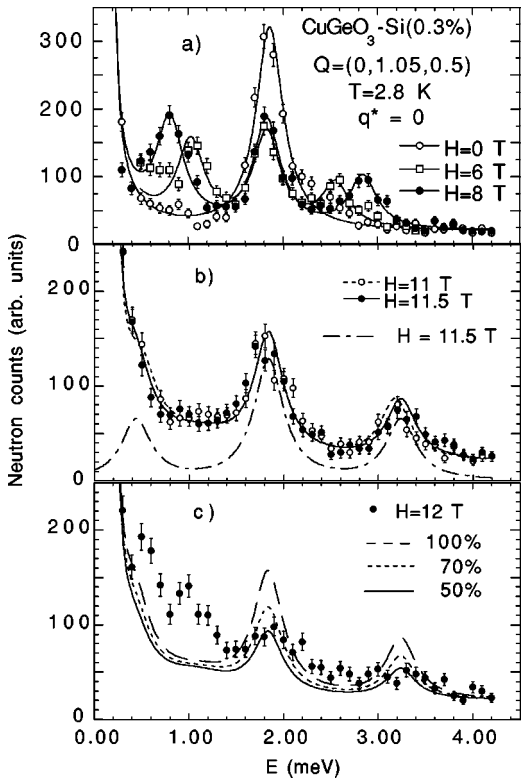

FIG. 11. Field effects on the excitation mode near the AF wave vector $\mathbf{Q}_{\mathrm{AF}}=(0,1,1/2)$ (i.e., $q^*=0$) in the doped compound. (a) The Zeeman splitting of the magnon mode in the D phase up to $H=8$ T. (b) Same as (a) for $H=11$ and 11.5 T ($H<Hc$). (c) In the I phase at $H=12$ T ($H>H_c$). The lines are explained in the text.

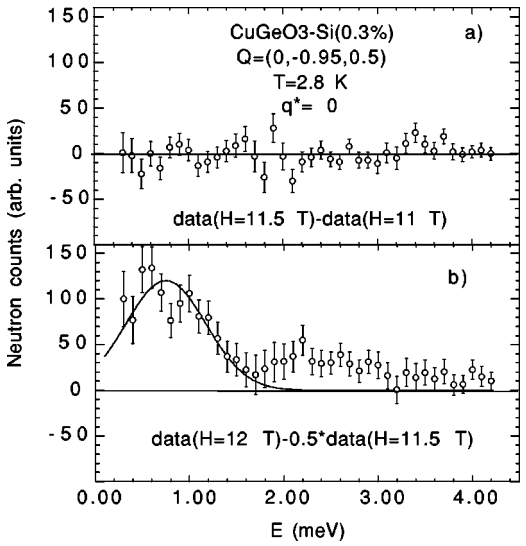

FIG. 12. Differential analysis between data obtained in the doped compound (shown in Fig. 11). (a) [data($H=11.5$ T) $-$ data($H=11$ T)]. (b) [data($H=12$ T) -0.5 data(11.5 T)] (see text). The line describes the low energy mode attributable to the I phase.

spinon continuum. Experimentally, the observed shift of the lower-energy boundary is in good agreement with the theoretical prediction of the simple model: $\delta_- = -g\mu_B H$. It is worth realizing that this specific ''Zeeman'' effect on a low-q spinon mode is related to the field-induced dynamical incommensurability which plays a so crucial role in the SP phenomenon (it drives the incommensurate lattice distortion at T_{SP}). It is observed here in a relatively low field ($H<H_c$) because the low-q spinon modes are little affected by the thermal damping (δE_T).

V. FIELD EFFECTS IN THE *I* PHASE

In the mixed compound $CuGe_{(1-x)}Si_xO_3$ with $x\simeq 0.003$, H_c occurs slightly below 12 T (see below). Such a small amount of impurities or defects in a SP system affects little the phase diagram.[32] The critical field value H_c is, however, reduced.[33] The static properties characterizing the I phase in this crystal have been previously investigated.[11] In particular, the superlattice peak [at $\mathbf{Q}_{k_{\mathrm{SP}}}=(1/2,0,1/2)$ in the D phase] is seen to be shifted apart from its commensurate position ($q^*=0$) along the $\mathbf{c}^*$ axis. In Ref. 11, for $H=12$ T, this shift is evaluated to be $\delta q = d/2\pi \simeq 0.007$ r.l.u. In our case, however, it is expected to be a bit smaller as the chosen field direction ($H\|a$) gives rise to a slightly larger critical field. Accordingly, for the same field value, the magnetization $\tilde{m}$ is smaller giving rise to a slightly smaller δq. Concerning the spin dynamics, our investigation has been performed on the instrument IN14. In Figs. 11(a) and 11(b), we consider first the Zeeman effect on the magnon mode at $\mathbf{Q}_{\mathrm{AF}}$ in the D phase (i.e., $H<H_c$). The solid line for $H=0$ accounts for the background, the incoherent inelastic scattering at low energy, and the acoustic magnon mode. The latter contribution is described by a simple function peaked at $E_{g1}\simeq 1.85$ meV, which defines the magnon gap of the D phase. For $H\neq 0$, taking into account the Zeeman splitting (with $\Delta E_z/H = 0.124$ meV/T), the same model [shown by the solid lines in Figs. 11(a) and 11(b)] provides similar good agreements with all the data up to H=11.5 T [the dot-dashed line in Fig. 11(b) displays the magnetic contribution at 11.5 T]. For $H=12$ T, however, the same simple model fails completely to explain the data [see the dashed line in Fig. 11(c)]. Our first claim is that, for this field direction, $11.5<H_c<12$ T. Second, since at $H=12$ T we are only slightly above H_c, hysteresis effects remain important ($\delta H\simeq 1$ T [11]). In such a case, two different behaviors, typical of the D and I phases, are expected to coexist in a ''mixed'' phase. The short-dashed and solid lines in Fig. 11(c) provides examples of a relative D-like contribution (expressed in % of the whole phase). Compared to the experiments, the residual peak observed around 1.85 meV is reasonably well explained if 50% of the magnetic contribution is attributed to the D-like behavior. To push further the analysis, we refer now to the differential method. First, we proceed to a test of the method. The data obtained in the D phase for the two close field values $H=11$ and 11.5 T [see Fig. 11(b)] are analyzed in Fig. 12(a). The differential method reveals no particular contribution, in excellent agreement with the fact that, within the statistics, the two sets of data are about the same. Second, we compare the data obtained at $H=12$ T with respect to the data obtained in the D phase at $H=11.5$ T. In the subtraction procedure, however, we reduce the expected contribution from the D phase (i.e., evaluated at $H=11.5$ T) by a factor of the order of 2. The data reported in Fig. 12(b), correspond to a model where 50% would result from the

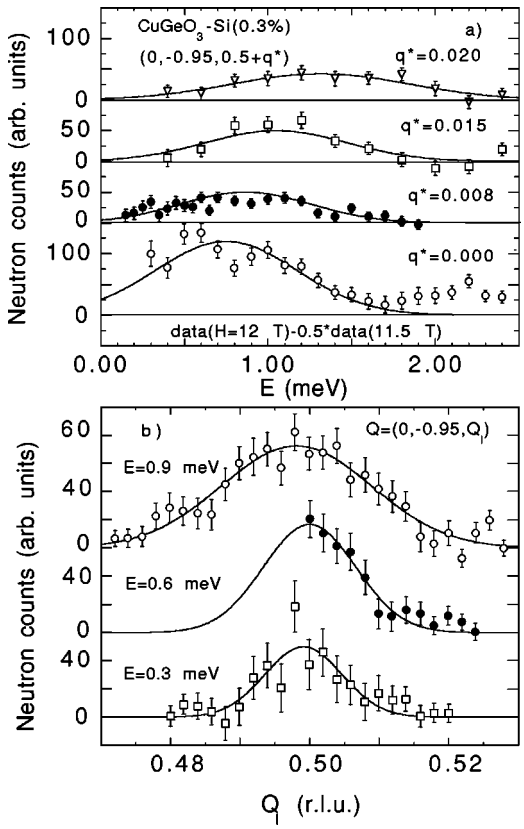

FIG. 13. Differential analysis [data($H=12$ T) -0.5 data($H=11.5$ T)]: (a) from energy scans showing the q dependence of the low-energy mode attributable to the I phase; (b) from Q_l scans at different energies (see text).

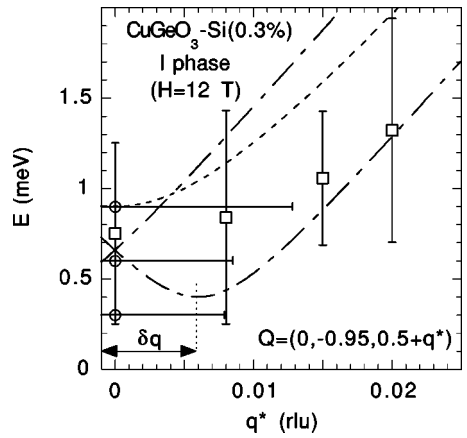

FIG. 14. Energy diagram of the low-energy excitations of the I phase as a function of q^*: experiments versus a prediction given by Hamiltonian (5). $\delta q = d/\pi = 0.006$ r.l.u. represents the expected magnetic incommensurability. The lines are obtained from Hamiltonian (5) (see text).

D-like contribution. These data can be considered as describing mainly the fluctuations of the I-like contribution. Essentially, they are characterized by a relatively broad contribution peaked at low energy $\simeq 0.7$ meV. Similar differential analyses have been developed on energy scans performed at different fixed wave vectors ($q^* \neq 0$) [see Fig. 13(a)]. With q^* increasing, the low energy peak is seen to be shifted to higher energies. In Fig. 13(b), Q_l scans performed at fixed energies are reported. They show that the energy spectrum broadens as q^* increases. The position of the different peaks observed in those figures are reported in Fig. 14, together with the corresponding experimental widths (shown by the vertical and horizontal segments). This figure reports new features. They can be considered as displaying the energy diagram of low-energy excitations in the I phase.

As proposed in Ref. 34, an oversimplified Heisenberg spin model can also be used to analyze such a I phase. Due to the incommensurate lattice distortion, an incommensurate modulation of the exchange coupling is to be expected and the spin Hamiltonian can be written as:

$$H = J^{\parallel} \Sigma_n [1 - \delta_1 \cos(2\pi q^*_{\rm inc} n)] \mathbf{s}_n \cdot \mathbf{s}_{n+1} \qquad (5)$$

where δ_1 is, as before, the ''alternation'' parameter and $q^*_{\rm inc}$ the incommensurate wave vector characterizing the magnetic exchange modulation along the chain. $q^*_{\rm inc}$ is entirely determined by the magnetization value $\tilde{m}$, with $q^*_{\rm inc} = 1/2 - d/2\pi$ where d characterizes the incommensurate lattice distortion. Considering the excitation spectrum, such an Hamiltonian predicts the occurrence of magnetic incommensurabilities (as in the U phase) and energy gaps. The results shown in Fig. 14 support the presence of a gap ($E_{gI} \simeq 0.7$ meV), but the incommensurability in the excitation spectrum is not explicitly observed. It could be shown, however, that our results do not contradict the predictions of Hamiltonian (5). As a very tentative example, possible longitudinal and transverse dispersions for this model are represented in Fig. 14 by the dotted and dot-dashed lines, respectively. The incommensurability has been fixed at $\delta q = d/\pi = 0.006$ r.l.u., which, as explained above, should be slightly smaller than the experimental determination 0.007 r.l.u. obtained in Ref. 11 (due to the different field orientation). In the model of Hamiltonian (5), the excitation branches are also characterized by energy gaps. In Fig. 14, the longitudinal and the (two) transverse branches are calculated for the following gap values: $\Delta_0 = 0.4$ meV and $\Delta_+ \simeq \Delta_- = 0.9$ meV, respectively. For the excitation velocity, we used the value $C_I = 14.7$ meV/r.l.u., which corresponds to the spinon velocity determined in the undoped compound.

VI. CONCLUSION

The effects of a magnetic field H are of crucial importance in the three U, D, and I phases of a SP system. As shown here, H acts directly on the spin excitations. In the U phase, there exists a sort of a ''competition'' between the thermal fluctuations and the field-induced dynamical incommensurability. This concerns the fluctuations near $\mathbf{Q}_{\rm AF}$. The low-q spinon modes, however, are seen to be little affected by these thermal fluctuations. Accordingly, the effect of H on these modes can be detected even at ''low'' field (i.e., $H < H_c$). At this point, an interesting comparison can be made with the results provided by electron spin resonance (ESR). By this technique, the uniform spinon mode [at $\mathbf{Q}_0 = (0,0,0)$, i.e., $q = 0$] is detected.[35] In a U phase ($T < T_{\rm max}$), the ESR resonance field measures directly the Zeeman shift which develops at $q = 0$ in the transverse fluctuation spectrum [see Fig. 7(b)]. This Zeeman effect is related to the induced dynamical incommensurability characterizing the field effect in a U phase. Concerning the D phase, one is

allowed to conclude that, in $CuGeO_3$, the field-induced Zeeman splitting develops in the whole Brillouin zone. This is to be opposed to what is observed in anisotropic $S=1$ Haldane spin chains.[22] A similar Zeeman splitting in the whole Brillouin zone has been observed in a $s=3/2$ spin system.[36] Such a difference between integer and half-integer spins could be a general feature of quantum gapped spin systems. For the *I* phase, our study in the doped compound is to be considered as a (very) preliminary investigation of the spin dynamics. In particular, no evidence is obtained for the expected dynamical incommensurability.[34] The presence of a low-energy gap, however, is convincingly established. Finally, along this work, reference is made to very simple isotropic Heisenberg hamiltonians. More realistic models should now be considered. In particular, in the strong spin-lattice coupling limit, which is now proposed to describe $CuGeO_3$,[5] the effects of a magnetic field on the elementary excitations may appear as a crucial test.

[1] For a review, see J. W. Bray, L. V. Interrante, I. S. Jacobs and J. C. Bonner, in *Extended Linear Chain Compounds*, edited by J. S. Miller (Plenum Press, New York, 1983), Vol. 3, and references therein.

[2] M. Hase, I. Terasaki, and K. Uchinokura, Phys. Rev. Lett. **70**, 3651 (1993).

[3] For a partial review on experimental results, see J.P. Boucher and L.P. Regnault, J. Phys. I **6**, 1939 (1996).

[4] G.S. Uhrig, Phys. Rev. B **57**, R14 004 (1998); R.J. Bursill, R.H. McKenzie, and C.J. Hamer, Phys. Rev. Lett. **83**, 408 (1999).

[5] C. Gross and R. Werner, Phys. Rev. B **58**, R14 677 (1998).

[6] M. Braden, B. Hennion, W. Reichardt, G. Dhalenne, and A. Revcolevschi, Phys. Rev. Lett. **80**, 3634 (1998).

[7] A recent work on the $(H-T)$ phase diagram can be found in J. Zeman, G. Martinez, P.H.M. van Loosdrecht, G. Dhalenne, and A. Revcolevschi, Phys. Rev. Lett. **83**, 2648 (1999), and references therein.

[8] A. Revcolevschi and G. Dhalenne, Adv. Mater. **5**, 9657 (1993); G. Dhalenne, J.C. Rouchaud, A. Revcolevschi, and M. Fedoroff, Physica C **282-287**, 953 (1997).

[9] L.P. Regnault, M. Aïn, B. Hennion, G. Dhalenne, and A. Revcolevschi, Phys. Rev. B **53**, 5579 (1996).

[10] L.P. Regnault, J.P. Renard, G. Dhalenne, and A. Revcolevschi, Europhys. Lett. **32**, 579 (1995).

[11] B. Grenier, L.P. Regnault, J.E. Lorenzo, J. Voiron, J. Bossy, J.P. Renard, G. Dhalenne, and A. Revcolevschi, Europhys. Lett. **44**, 511 (1998).

[12] M. Braden, G. Wilkendorf, J. Lorenzana, M. Aïn, G. McIntyre, M. Behruzi, G. Dhalenne, and A. Revcolevschi, Phys. Rev. B **54**, 1105 (1996).

[13] T.M. Brill, J.P. Boucher, J. Voiron, G. Ghalenne, and A. Revcolevschi, Phys. Rev. Lett. **73**, 1545 (1994).

[14] V. Kiryukhin, B. Keimer, J.P. Hill, and A. Vigliante, Phys. Rev. Lett. **76**, 4608 (1996).

[15] M. Nishi, O. Fujita, and J. Akimitsu, Phys. Rev. B **50**, 6508 (1994).

[16] G. Castilla, S. Chakravarty, and V.J. Emery, Phys. Rev. Lett. **75**, 1823 (1995); J. Riera and A. Dobry, Phys. Rev. B **51**, 16 098 (1995).

[17] G. Bouzerar, Ö. Legeza, and T. Ziman, Phys. Rev. B **60**, 15 278 (1999).

[18] Different models have been proposed, see, for instance, I. Yamada, M. Nishi, and J. Akimitsu, J. Phys.: Condens. Matter **8**, 2625 (1996) and Ref. 19.

[19] J.E. Lorenzo, L.P. Regnault, J.P. Boucher, B. Hennion, G. Ghalenne, and A. Revcolevschi, Europhys. Lett. **45**, 619 (1999).

[20] G.S. Uhrig and H.J. Schulz, Phys. Rev. B **54**, 9624 (1996).

[21] O. Fujita, J. Akimitsu, M. Nishi, and K. Kakurai, Phys. Rev. Lett. **74**, 1677 (1995).

[22] L.P. Regnault, I. Zalizniak, J.P. Renard, and C. Vettier, Phys. Rev. B **50**, 9174 (1994).

[23] In the simplified energy diagram of Fig. 1(b), the gap E_{g2} occurs also at $Q=(0,1/2)$.

[24] G.S. Uhrig, Phys. Rev. Lett. **79**, 163 (1997).

[25] G. Muller, H. Thomas, H. Beck, and J.C. Bonner, Phys. Rev. B **24**, 1429 (1981).

[26] L.D. Faadev and L.A. Takhtajan, Phys. Lett. **85A**, 375 (1981).

[27] H.J. Schulz, Phys. Rev. B **34**, 6372 (1986).

[28] K. Fabricius, U. Lowe, and J. Stolze, Phys. Rev. B **55**, 5833 (1997).

[29] S. Sachdev, Phys. Rev. B **50**, 13 006 (1994).

[30] M. Braden, B. Hennion, P. Pfeuty, G. Dhalenne, and A. Revcolevschi, Phys. Rev. Lett. **83**, 1858 (1999).

[31] M. Arai, M. Fujita, M. Motokawa, J. Akimitsu, and S.M. Bennington, Phys. Rev. Lett. **77**, 3649 (1996).

[32] B. Grenier, L.P. Reganult, J.E. Lorenzo, J. Voiron, J. Bossy, J.P. Renard, G. Ghalenne, and A. Revcolevschi, Phys. Rev. B **57**, 3444 (1998).

[33] In presence of impurities, a three-dimensional magnetic ordering occurs at low temperature (T_N). Such an effect has been widely investigated in the *D* phase. It occurs also in the *I* phase. All the measurements discussed in the present work have been obtained at $T>T_N$.

[34] G.S. Uhrig, F. Schönfeld, and J.P. Boucher, Europhys. Lett. **41**, 431 (1998).

[35] J.P. Boucher, L.P. Regnault, and L.E. Lorenzo, RIKEN Rev. **24**, 5 (1999).

[36] B. Leuenberger, H.U. Güdel, R. Feile, and J.K. Kjems, Phys. Rev. B **31**, 597 (1985); B. Leuenberger, J. Phys. C **19**, 4083 (1986).